

To Ask or Not to Ask?

Detecting Absence of Information in Vision and Language Navigation

Savitha Sam Abraham*, Sourav Garg*, Feras Dayoub*

* Australian Institute for Machine Learning
The University of Adelaide

{savitha.samabraham, sourav.garg, feras.dayoub}@adelaide.edu.au

Abstract

Recent research in Vision Language Navigation (VLN) has overlooked the development of agents' inquisitive abilities, which allow them to ask clarifying questions when instructions are incomplete. This paper addresses how agents can recognize "when" they lack sufficient information, without focusing on "what" is missing, particularly in VLN tasks with vague instructions. Equipping agents with this ability enhances efficiency by reducing potential digressions and seeking timely assistance. The challenge in identifying such uncertain points is balancing between being overly cautious (high recall) and overly confident (high precision). We propose an attention-based instruction-vagueness estimation module that learns associations between instructions and the agent's trajectory. By leveraging instruction-to-path alignment information during training, the module's vagueness estimation performance improves by around 52% in terms of precision-recall balance. In our ablation experiments, we also demonstrate the effectiveness of incorporating this additional instruction-to-path attention network alongside the cross-modal attention networks within the navigator module. Our results show that the attention scores from the instruction-to-path attention network serve as better indicators for estimating vagueness.

1. Introduction

Vision Language Navigation (VLN) is the task of enabling a robot to navigate an environment based on a given instruction. There has been substantial research in VLN in the recent past [25]. The majority of previous research has focused on training large neural models for VLN task using synthetic datasets like R2R [2] that contained step-by-step instructions and Reverie [16] that had high-level instructions, among others. All these models operate under the assumption that agents are designed to act independently without human intervention. Even when dealing with ab-

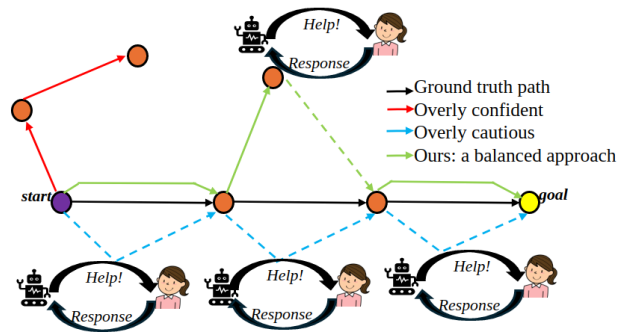


Figure 1. Navigation agent paths using different instruction-vagueness estimation approaches: (1) Overly confident approach (red) that rarely seeks help, (2) Overly cautious approach (blue) that seeks help very often and (3) Our balanced approach (green) that seeks timely assistance. Dashed arrows indicate movements made with external assistance (best viewed in color).

stract or high-level instructions, agents are trained to explore and make decisions they deem best for progressing towards their goals. There is no provision for indicating uncertainty or indecision about the next course of action. Typically, designers impose an upper time limit in these approaches, prompting agents to cease operations after a pre-defined number of moves, regardless of goal achievement.

When a robot transitions to a real-world environment, it often encounters instructions from various individuals, each with unique communication styles. Adapting to this diversity poses a challenge in generalizing across different instructing styles. While some individuals may prefer concise instructions, others might delve into details but present them in a disorganized manner. A second person unfamiliar with the instructor may find it challenging to follow the instructions easily. In such situations, humans typically seek clarification by asking questions like, "I'm now in front of the kitchen. Where should I go next?". Implementing a similar ability is a desired feature in intelligent robots to tackle uncertainty due to vagueness in the input instruction.

When a robotic agent is posed with an unclear instruction, it may get stuck at some point, or it may keep exploring, taking very long paths before reaching the goal, or it may never reach the goal. Rather than waiting for the robot to encounter failure, it is preferable if the robot can be proactive and seek help when it is approaching failure.

We are interested in the task of Under-specified Vision Language Navigation (ULN) as outlined in [8]. ULN introduced a nuanced modification to the VLN task by incorporating a new dimension of information completeness. In this paper, we focus on the task of instruction-vagueness estimation within the context of ULN. Instruction-vagueness (IV) estimation assesses the uncertainty arising from vague input instructions in the decision-making process of a VLN agent. In essence, an IV estimation module addresses the VLN agent’s query: “*Do I possess enough information to proceed with my next move or do I seek assistance?*”. A key requirement for this module is to find the right balance (see Figure 1) between being overly cautious and frequently seeking help, which guarantees task completion (high recall), and being overly confident, potentially resulting in excessive exploration without finishing the task (high precision). The contributions of this paper are as follows:

- We introduce an attention-based **instruction-vagueness (IV) estimation** module and integrate it into an existing VLN model. The module takes the instruction, the path followed thus far, and the proposed next move as its inputs and decides at each time step *whether to follow the VLN model’s suggestion or to request assistance*.
- We introduce a **pre-training task** that helps *identify important parts of the instructions needed for predicting actions*. By incorporating this instruction to path alignment information into the Instruction-Vagueness (IV) module, we significantly improve its ability to detect points of uncertainty, enhancing precision-recall balance.

2. Related Work

In this section we provide a brief survey of recent works related to vision language navigation and uncertainty arising from vagueness in input instruction.

2.1. Vision Language Navigation

Existing methods in VLN vary depending on the information used to predict the next location to move to. Chen et al. [3] introduced HAMT (History Aware Multimodal Transformer), a framework that retains a record of all previously visited and observed locations as historical data. This information, along with the input instruction is then utilized to determine the next destination, typically chosen

from among the neighboring locations of the current position. VLN-DUET (Dual Scale Graph Transformer), as described in [5], employs a detailed representation of the current observation derived from objects in the image instead of a coarse representation of the current location. Additionally, it also maintains a topological map of the nodes visited thus far as in [3] to determine the subsequent node for navigation. This next node may include any unvisited nodes observed thus far, expanding beyond the immediate local neighbors (performing global action planning). Recent studies aim to create large-scale VLN datasets [4, 18] to enhance the generalizability of VLN agents. Speaker follower models [9] and instruction following and generation models [24] focus on refining instruction generation and interpretation abilities of the agent. Numerous researchers have also made significant efforts to enhance vision-language alignment in VLN by introducing a variety of pre-training tasks [7], [6], [26]. With the emergence of Large Language Models (LLMs), recent advancements in VLN have increasingly incorporated LLMs in navigation [17, 27].

In this paper, we evaluate the effectiveness and generalizability of our proposed IV estimation module by incorporating it into two navigators, VLN-DUET and HAMT. We first examine how well these navigators, trained with detailed instructions from the R2R dataset [2], adapt to vague instructions. We integrate our IV estimation module into both to *recognize potential absence of critical information*, prompting them to seek assistance.

2.2. Knowing when you don’t know

ULN [8] as mentioned in Section 1, introduced the dataset based on R2R for the problem of under-specified VLN. ULN modified the R2R dataset by adding a high-level instruction, that intentionally omitted certain details, alongside the original fine-grained instruction for each trajectory. These high-level, vague instructions corresponding to the fine-grained instructions were manually created and validated. The paper handled vagueness in instruction by introducing two separate modules - an instruction classifier and an uncertainty estimation module. The instruction classifier classified an instruction as either high or low level. The uncertainty estimation module predicts a score indicating the uncertainty of the next move, using candidate moves weighted by likelihood and attention scores. In this paper, we introduce an attention-based IV estimation module that assesses the uncertainty arising from instruction vagueness in the predictions of a VLN model. We demonstrate that the alignment between the given instruction and the path taken so far is an effective metric for gauging IV. In contrast to the approach in [8], where an instruction classifier labels an instruction as low or high-level (indicative of potential vagueness) based solely on the instruction content, we contend that *vagueness arises not merely from the instruction*

itself, but from the interaction between the instruction and the surrounding environment.

Vision Dialog Navigation (VDN) involves enabling robots to seek help during navigation [22]. A related work [28] introduced an MLP-based uncertainty estimator that identified uncertainty points based on the navigator’s current state and was trained using pseudo-labels of uncertainty derived from the entropy of the navigator’s predicted distribution. We compare this with our IV model, which uses instruction-path attention, and show that our approach more accurately indicates uncertainty and generalizes across different navigators. We demonstrate that relying on the predicted distribution’s entropy can be misleading, as the navigator might confidently make incorrect predictions about the next move.

Another recent work that explored uncertainty estimation is *KnowNo* [19]. It utilised conformal prediction to gauge uncertainty in the next-step prediction of a LLM-based planner. Uncertainty due to instruction ambiguity is studied in *CLARA* [15], where a LLM-based framework was used to discern whether a provided user input instruction is ambiguous or infeasible. It adopts the method of self-consistency check involving sampling multiple responses from the LLM for the same query, and assessing the consistency among these responses. This approach is similar to the conventional ensemble method for uncertainty estimation [12]. It is not efficient to implement an ensemble-based approach for VLN considering the complexity of the task, which typically comprises individual networks for text encoding, image encoding, topological graph encoding and cross-attention. It requires training all these layers or a selected sub-network (text encoder) as done in [8] separately, freezing all other layers. Our aim here is to avoid re-training any part of the VLN model, and limit the training to just the IV module.

3. Method

3.1. Problem Background and Formulation

In a VLN setup for discrete environments, the environment at any time step t is represented as an undirected graph $G_t = (V_t, E_t)$. G_t represents the map of the environment explored so far with $V_t = \{N_i\}_{i=1}^K$, being the set of nodes or locations observed so far and E denoting the connectivity between the locations. Nodes are flagged as either visited or navigable (potential next nodes). The graph starts with the agent’s initial position and updates at each time step to include the current position and new navigable nodes.

The input instruction $I = \{w_i\}_{i=1}^L$ is a sequence of word embeddings, with L words. The agent’s goal is to navigate from its current position to the goal location described in the instruction. The VLN model includes a text encoder f_{text} (typically a multi-layer transformer) that generates context-

ual representation of the instruction, \hat{I} . The agent also has a cross-attention network, $f_{\text{cross-attention}}$, that learns a graph-aware and instruction-aware representation for each node in the graph, represented as $\hat{G}_t = (\hat{V}_t, E_t)$. It also learns the attention weights of visual inputs on language, represented as α_t . The action predictor network, $f_{\text{actionPredictor}}$ predicts the subsequent node the agent will move to at each time step by assigning a likelihood score to each navigable node in \hat{G}_t , represented as β_t .

$$\hat{I} = f_{\text{text}}(I) \quad (1)$$

$$\hat{G}_t, \alpha_t = f_{\text{cross-attention}}(\hat{I}, G_t) \quad (2)$$

$$\beta_t = f_{\text{actionPredictor}}(\hat{I}, \hat{G}_t) \quad (3)$$

$f_{\text{actionPredictor}}$ thus predicts the next node to move to at each time step, eventually resulting in a sequence of nodes or the path, $P = \{N_i\}_{i=1}^{L_p}$, traversed by the agent to execute the task. L_p is the length of the path generated. The segment of the path traversed up to time t is denoted by P_t .

An Instruction-Vagueness (IV) estimation module, f_{IV} , computes for each time step, t , the uncertainty, $\text{score}_t^{\text{uncertainty}}$, arising from vagueness in the instruction, \hat{I} , in the prediction of β_t by $f_{\text{actionPredictor}}$.

3.2. Our approach: Instruction Vagueness Estimation

The architecture of f_{IV} is shown in Figure 2. The vagueness in instruction at any point during traversal is modeled as a function of both the instruction and the path being undertaken. If node \hat{N}_t is predicted as the most likely node to move to at time step t by $f_{\text{actionPredictor}}$,

$$\bar{P}_t = P_{t-1} + \hat{N}_t \quad (4)$$

$$\text{score}_t^{\text{uncertainty}} = f_{\text{IV}}(\bar{P}_t, \hat{I}) \quad (5)$$

Here, P_{t-1} denotes the path taken by the agent until time $(t - 1)$. Appending \hat{N}_t , the next move suggested by $f_{\text{actionPredictor}}$ to it gives \bar{P}_t , the most likely path up to time t . The goal of f_{IV} is to determine the uncertainty arising from instruction vagueness in the prediction of $f_{\text{actionPredictor}}$. f_{IV} employs a multi-head attention (MHA) network [23] to learn the alignment between this anticipated path at time t and the instruction.

$$\text{Instr_Path_Attn}_t = \text{MultiHead}(\hat{I}, \bar{P}_t, \bar{P}_t) \quad (6)$$

$$\text{MultiHead}(\hat{I}, \bar{P}_t, \bar{P}_t) = \text{Concat}(\text{head}_1, \dots, \text{head}_h)W^O \quad (7)$$

$$\text{head}_i = \text{Attention}(\hat{I}W_i^Q, \bar{P}_tW_i^K, \bar{P}_tW_i^V) \quad (8)$$

$$\text{Attention}(\hat{I}, \bar{P}_t, \bar{P}_t) = \text{softmax}\left(\frac{\hat{I}(\bar{P}_t)^T}{\sqrt{d_k}}\right)\bar{P}_t \quad (9)$$

Here, Instr_Path_Attn_t is an enhanced representation that captures the alignment between \hat{I} and the likely path,

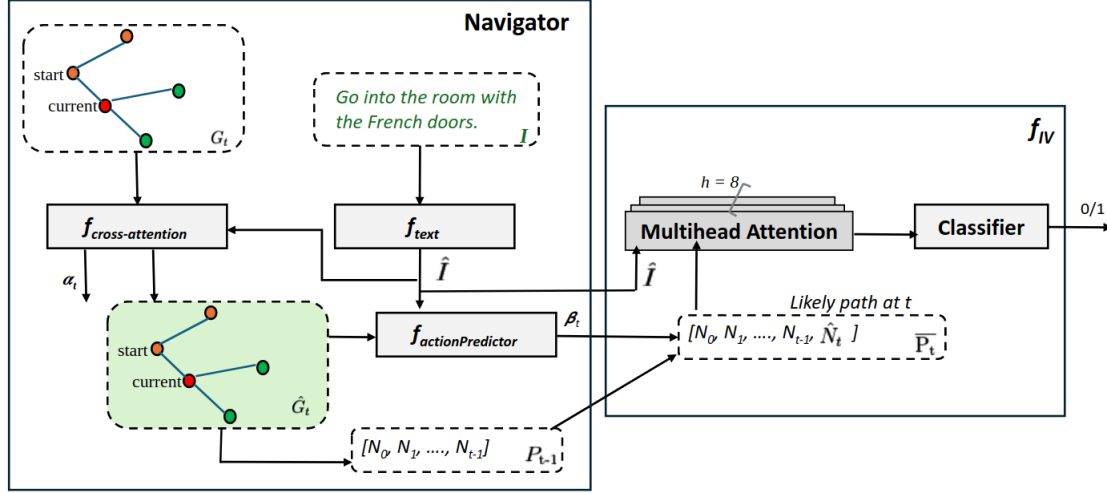


Figure 2. Interaction between the navigator and the IV module: The IV module receives the encoded instruction and the path taken so far with a suggestion for the next move from the navigator. It predicts the certainty in the navigator’s next move suggestion.

\overline{P}_t . W_i^Q, W_i^K, W_i^V are learned projection matrices for each attention head i , W^O is a learned output projection matrix, h denotes the number of attention heads ($= 8$), and d_k represents the dimensionality of the instruction embedding ($= 768$). The enhanced representation, $Instr_Path_Attn_t$, is then passed onto a binary classifier, a linear transformation layer that produces two scores for the two classes “certain” and “uncertain”.

$$score_t^{\text{uncertainty}} = W \cdot Instr_Path_Attn_t + b \quad (10)$$

where W is a $2 \times d_k$ weight matrix, and b is the bias. If $score_t^{\text{uncertainty}}$ indicates “uncertainty”, the agent is prompted to seek assistance; otherwise, it proceeds with the suggested move. In this study, we assume the existence of an oracle in place of a human who provides assistance. When the agent requests assistance, this oracle provides the optimal move — the one that guides the agent along the shortest path to its goal from its current position.

Supervision: Training f_{IV} network requires ground truth labels indicating whether the prediction made by $f_{\text{actionPredictor}}$ is uncertain ($= 1$) or not ($= 0$). Since, we do not have these labels, we approximate it in two ways.

- **Based on ground truth path ($label_{GP}$):** If the move predicted by the VLN agent at time step t is same as the ground truth move at t , it is considered “certain”, else, uncertain. This way of approximating uncertainty labelling is commonly observed in literature [8].
- **Based on instruction-path alignment ($label_{IP}$):** In this paper, we explore using instruction-to-path alignment for uncertainty labeling. This approach assumes the existence of information about instruction-to-path

alignment, which associates each node in the path with a specific sub-instruction. Given a ground truth path, $GP = \{N_0, N_1, \dots\}$ and each instruction represented as a list of sub-instructions, $SI = \{S_1, S_2, \dots, S_m\}$, the instruction to path alignment maps GP to SI . This mapping is denoted as $Rel_SI(N_t)$, which returns the sub-instruction from SI that is aligned with N_t in GP . This mapping is utilized to label uncertainty arising from instruction vagueness as follows:

$$uncertainty_t = \begin{cases} 0 & \text{if } Rel_SI(N_t) \text{ in input instruction} \\ 1 & \text{otherwise} \end{cases} \quad (11)$$

In essence, this labeling checks at each time step whether the relevant sub-instruction is present in the input instruction. If not, it indicates that the input instruction is vague and lacks necessary information relevant for making the prediction at that point.

Loss function: The loss function used in either case is the binary cross entropy loss (BCE) [20].

3.3. Pre-training task: Relevant Instruction Span Identification

We propose a pre-training task that serves to initialize the weights of the multihead attention network in f_{IV} . The task is a instruction to path alignment task. The objective of this task is to predict the segment/chunk of the instruction that is most relevant when predicting the agent’s move at time-step t , given the path taken so far, P_t . It is formulated as a sequence-to-sequence classification problem, where each token in the input instruction is classified as 0 or 1 based on

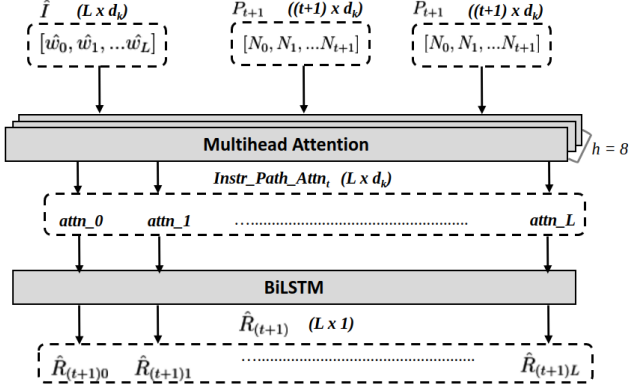


Figure 3. Pre-training: Architecture of the network that learns to identify the most relevant span or chunk in \hat{I} that influenced the last move made, N_{t+1} .

its relevance. The task is defined as:

$$\hat{R}_t = f_{\text{pretrainAlign}}(P_t, \hat{I}) \quad (12)$$

In this context, \hat{I} , a $L \times d_k$ dimensional representation of the instruction, is transformed into a $L \times 1$ dimensional relevance sequence. L denotes the number of tokens in the instruction. The output sequence indicates the relevance of each token (assigned 1 if relevant, otherwise 0) in predicting the move at time step t .

The architecture of the network for the pretraining task is illustrated in Figure 3. It consists of a multihead attention layer followed by a BiLSTM network [11] that maps the refined representation that incorporates instruction to path alignment information, to the relevance sequence [21]. We opt for a BiLSTM rather than a more complex transformer model due to data limitations.

Supervision: We leverage the instruction to path alignment information in the dataset, Fine-Grained R2R (FGR2R) [10], for training $f_{\text{pretrainAlign}}$. Each fine-grained instruction I_{orig} in FGR2R is segmented into sub-instructions or chunks and each node from the ground truth path is mapped to the most relevant sub-instruction within the instruction. Such a mapping, denoted as $Rel_SI(N_t)$, provides information about the sub-instruction from I_{orig} that is aligned with any node N_t in the ground truth path. The network, $f_{\text{pretrainAlign}}$, is trained independently, keeping the weights of the different components in the navigator - f_{text} , $f_{\text{cross-attention}}$ and others frozen. It may be noted that the navigator acts in a teacher-forcing manner - that is, the move it makes at any time t is always the ideal move or the move at time step t in the ground truth path. This is because, the instruction-path alignment information in FGR2R is with respect to the ground truth paths in the dataset.

Loss function: The network is trained using a combination of BCE loss and Dice loss [14]. While BCE loss ensures ac-

curate probability prediction for each token independently, Dice loss encourages accurate identification of boundaries of relevant span within the instruction.

4. Experiments

4.1. Research Questions

The following are the research questions we aim to address through our experiments:

1. **RQ1:** How does the performance (precision-recall balance) of our proposed instruction-to-path attention-based instruction vagueness estimator compare to existing approaches?
2. **RQ2:** How does utilizing different pseudo-labels for uncertainty - $label_{IP}$, $label_{GP}$ and entropy-based label affect the performance of IV module?
3. **RQ3:** Does incorporating instruction to path alignment knowledge through pre-training of multi-head attention layer improve the performance of IV module?

4.2. Dataset

The original R2R dataset [2] is divided into four principal splits: `train`, `val_seen`, `val_unseen`, and `test`. The `val_seen` split contains environments similar to those in the `train` split, whereas `val_unseen` and `test` feature trajectories in entirely new, unobserved environments. The ULN dataset [8], features a manually created coarse-grained or high-level instruction, I_{short} , along with the original fine-grained instruction, I_{orig} for each trajectory in `val_seen` and `val_unseen`. We also utilize the instruction to path alignment information for each trajectory from the FGR2R variant of R2R [10]. Next, we describe the data used for training and evaluation in our experiments.

$f_{\text{pretrainAlign}}$ train/val data: $f_{\text{pretrainAlign}}$ training exclusively uses the `train` split of R2R, which comprises approximately 11,400 trajectories. We divide this training set into training and validation subsets in an 80 to 20 ratio and do not use trajectories from `val_seen` and `val_unseen` during pre-training.

f_{IV} train/val data: We train f_{IV} using approximately 2,000 trajectories from the `val_seen` split, providing I_{orig} as input instruction for 50% of the trajectories and I_{short} for the remainder. This approach ensures a balanced dataset enabling f_{IV} to discern between the two types of instructions during training.

f_{IV} test data: We evaluate our instruction vagueness estimator on trajectories in `val_unseen`, where I_{orig} is used as the input instruction for 50% of the trajectories and I_{short} for the remaining trajectories. We do not use the `test` split of R2R as it lacks annotation for I_{short} in it.

It is important to acknowledge that the data set available for training f_{IV} is limited as it is costly to manually annotate a given path with different styles of instructions.

4.3. Implementation Details

The model $f_{\text{pretrainAlign}}$ is trained for 7000 iterations with a batch size of 8, learning rate of $1e-4$. Equal weights are given to both dice and BCE loss. The model f_{IV} is trained for 1000 iterations with a batch size of 8, learning rate of $1e-4$. The model is trained on imitation learning. Both models are trained with AdamW optimizer [13] on a single GPU - NVIDIA GeForce RTX 4090.

4.4. Baseline

The uncertainty estimation module in [8] is defined as follows:

$$score_t^{\text{uncertainty}} = f_{\text{Base}}(\alpha_t, \beta_t) \quad (13)$$

α_t and β_t are as defined in Equations 2 and 3 in Section 3.1. This approach leverages α_t , the visual attention on instruction from the VLN model, and β_t , which are the likelihood scores that the VLN agent assigns to potential next moves at each time step. These two components are concatenated and fed into a classifier, which then assesses the uncertainty in the predictions made by the VLN model. The approach uses supervised learning with pseudo-labels for uncertainty derived from ground truth path - $label_{GP}$. We denote this method as f_{Base} . Comparing to f_{Base} enables us to assess whether the attention scores from the navigator serve as a better indicator of vagueness than the instruction-to-path attention scores learned by f_{IV} .

The next baseline is the uncertainty estimator used in VDN task [28], defined as:

$$score_t^{\text{uncertainty}} = f_{\text{VDN}}(\alpha_t) \quad (14)$$

Here, pseudo-labels for uncertainty are derived from the entropy of the navigator’s predicted distribution, β_t (if entropy is close to that of a uniform distribution, i.e., within a predefined threshold, $\epsilon \in [0, 1]$, it is considered uncertain). Comparing with f_{VDN} also allows us to evaluate the effectiveness of entropy as an uncertainty indicator versus using pseudo-labels based on the ground truth move $label_{GP}$ and alignment information $label_{IP}$.

The next baseline involves conformal prediction, as outlined in [19]. This method utilizes a calibration set to determine a threshold, θ , for the probability assigned to the most probable next move by the VLN agent. The threshold is set as a function of user-defined error tolerance (is set as 0.9 in our experiments). Moves are accepted if their probabilities fall within this threshold; otherwise, they are deemed uncertain. We denote this method as f_{CP} .

4.5. Evaluation Metrics

We evaluate the Instruction Vagueness (IV) module using a precision-recall balance metric:

$$\text{Balance} = \frac{\text{Precision} - \text{Recall}}{\text{Precision} + \text{Recall}} \quad (15)$$

Balance $\in [-1, 1]$; negative values indicate higher recall, positive values indicate higher precision, and 0 indicates a balance with Precision = Recall. The ground truth labels for uncertainty is based on $label_{GP}$.

Model	Instruction Style	SPL (%)	NE (m)
DUET	I_{orig}	54.46	3.86
	I_{short}	47.35	5.30
HAMT	I_{orig}	43.82	5.46
	I_{short}	31.58	7.11

Table 1. Generalization to coarse-grained or high-level instruction for DUET and HAMT.

Predicting ‘uncertain’ prompts the agent to seek help, opting for guidance from the oracle rather than following its original predicted move. This intervention can help redirect an agent that might be straying from the correct path back towards the intended route. We examine how assistance from the oracle enhances performance metrics such as Success Path Length (SPL) and Navigation Error (NE), which are standard metrics in VLN evaluations [1]. NE measures the distance between the agent’s final position and the target location in meters, while SPL evaluates both the success of reaching the target and the path efficiency.

4.6. Results

Our aim is not to outperform existing VLN models in SPL and NE but to address the issue of identifying information gaps during navigation. The improvement in SPL and NE are achieved with oracle assistance and is used as an indicator of timely assistance. We base our experiments on two VLN models, though we believe the IV module can be integrated into any VLN model with components as shown in Figure 2.

Generalization to coarse-grained or high-level instruction: Table 1 shows the performance of VLN models, DUET [5] and HAMT [3], trained on R2R dataset on f_{IV} test data. The first row shows the SPL and NE when I_{orig} is used as the input instruction for all the cases. The second row shows the results when I_{short} is used as the input instruction. We see a drop in performance, confirming that the models trained on a specific instruction style (I_{orig} style) struggle to generalize to a different instruction style (I_{short} style). It may also be noted that DUET performs better than HAMT in either cases.

Method	Model	SPL (%)	NE (m)	Precision (%)	Recall (%)	Balance	Orig/Short (%)
DUET	f_{CP}	96.40	0.24	36.4791	99.0147	-0.4615	100/100
	f_{Base}	52.10	4.04	72	11.1455	0.7319	28/33
	f_{VDN}	55.86	3.58	47.1962	15.2798	0.5108	64/65
	$f_{IV(GP)}$	57.86	3.51	62.5	14.5631	0.6220	30/42
	$f_{IV(GP+pretrain)}$	58.10	3.31	63.0681	17.5078	0.5654	40/46
	$f_{IV(IP)}$	75.24	2.16	37.5680	39.0566	-0.0194	26/79
HAMT	f_{CP}	88.34	1.29	54.4993	88.4773	-0.2376	100/100
	f_{Base}	67.29	3.34	64.8230	49.6610	0.1324	81/ 92
	f_{VDN}	38.38	5.63	41.5841	8.1237	0.6731	54/47
	$f_{IV(GP)}$	68.82	3.21	55.4414	48.6486	0.0652	89/89
	$f_{IV(GP+pretrain)}$	75.84	2.32	51.2520	58.1439	-0.0629	90/96
	$f_{IV(IP)}$	70.32	3.35	39.2733	45.0396	-0.0683	27/79

Table 2. Results comparing baselines f_{CP} , f_{Base} , f_{VDN} with different variants of the proposed IV module ($f_{IV(GP)}$ and $f_{IV(IP)}$): IV trained with pseudo-labels $label_{GP}$ and $label_{IP}$ respectively, $f_{IV(GP+pretrain)}$: IV with MHA initialized to pretrained weights and finetuned with pseudo-label $label_{GP}$) on VLN-DUET and VLN-HAMT. We highlight the best variant: highest SPL, lowest NE and best balance (value closest to 0), with more emphasis on balance.

As mentioned in Section 4.2, f_{IV} test data comprises a balanced dataset with respect to two instruction styles: 50% of instances have high-level instructions as input, denoted as $Inst_{short}$, and the remaining have fine-grained instructions as input, denoted as $Inst_{orig}$. It is important to note that while I_{orig} is fine-grained and contains more details than I_{short} , it may also benefit from additional details, as indicated by potential improvements that can be made in both SPL and NE with I_{orig} instructions (see Table 1). These results suggest that the generated paths differ from the ground truth paths.

The goal of IV module is to identify uncertain moves and reduce the drop that is seen in SPL and NE with the change in instruction style. For instance, with IV support, DUET is expected to achieve an SPL above 47.35 and NE below 5.30 when I_{short} is used as the input instruction. If effective, DUET with IV may reach an SPL higher than 54.46, surpassing the SPL with original fine-grained instructions, showing that timely assistance can guide the agent closer to the ground truth path.

Table 2 compares various variants of our proposed approach f_{IV} with baseline approaches, when integrated with two navigators - DUET and HAMT. The column *Orig/Short* shows the percentage of instances in each category ($Inst_{Orig}$ versus $Inst_{Short}$) where an oracle intervention was recommended by the instruction vagueness estimation module.

Comparing to baselines (RQ1): Table 2 illustrates that f_{CP} , an approach based on conformal prediction for uncertainty estimation, exhibits very high recall. It tends to be overly cautious, prompting intervention almost at every time-step, regardless of the input instruction style. This resulted in a high SPL and low NE.

Next, we compare f_{Base} with $f_{IV(GP)}$, a variant of f_{IV} . Both these models are trained with uncertainty labels based on ground truth paths ($label_{GP}$). It can be seen that both

models perform better with HAMT than with DUET. This can be attributed to the fact that HAMT makes more incorrect predictions and hence f_{Base} and $f_{IV(GP)}$ when integrated with HAMT, observes more cases of uncertainty during its training. The baseline f_{Base} , relying on attended representations α_t from the navigation model, shows more imbalance between precision and recall - with higher precision compared to recall, indicating excessive confidence in the navigation agent’s decisions at each time-step. The results indicate that incorporating an explicit attention network in f_{IV} to learn instruction-to-path attention representations improves precision-recall balance in uncertainty estimation compared to using the attended representation α_t from the navigation agent.

Comparing different pseudo-labels for uncertainty

(RQ2): We examine the impact of using uncertainty labels derived from instruction to path alignment information ($label_{IP}$) instead of those derived from ground truth paths ($label_{GP}$). To do this, we compare the models $f_{IV(GP)}$ and $f_{IV(IP)}$. A notable finding is the distinct treatment of instances from the two styles, with more instances of oracle intervention suggested in $Inst_{short}$ than in $Inst_{orig}$. This results from $label_{IP}$, which is not agnostic to the instruction-style. It influences the IV estimation module to associate “uncertain” label more with instructions of style I_{short} than with I_{orig} . However, I_{orig} may also benefit from additional details as shown in our experiments, refer Table 1. The significant increase in SPL and reduction in NE indicate its effectiveness in identifying uncertain points in $Inst_{short}$ trajectories more efficiently, striking a balance between precision and recall. This demonstrates that such instruction-to-path alignment information can be a better indicator to identify missing information in instructions at any given time point. DUET showed best results with the variant $f_{IV(IP)}$.

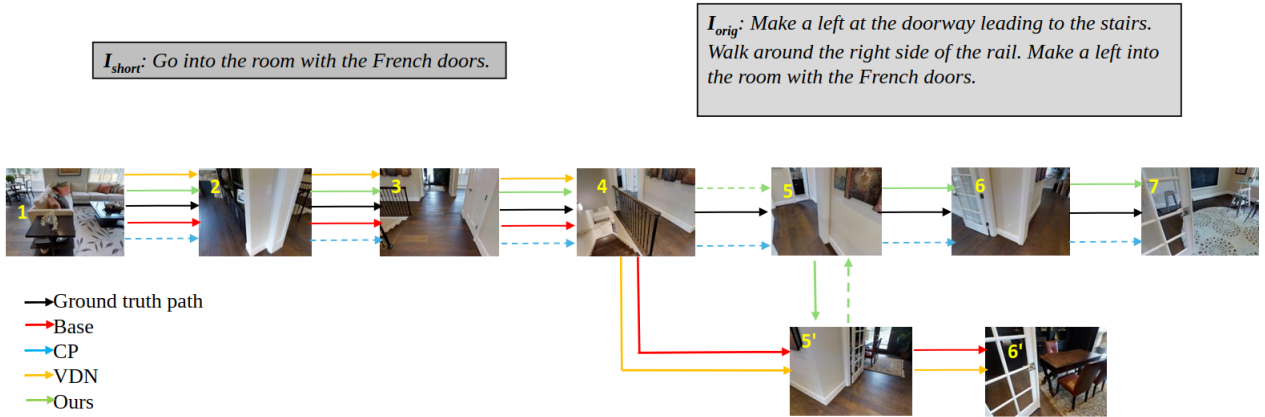


Figure 4. A navigation example with the input I_{short} showing the agent trajectories when supported by f_{CP} (blue), f_{Base} (red) and our approach $f_{IV(GP+pretrain)}$ (green). Dashed arrows indicate movements with oracle intervention (best viewed in color).

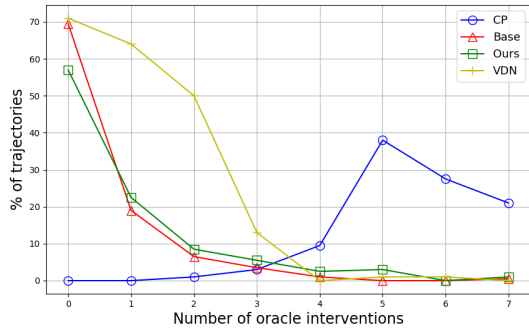


Figure 5. Number of oracle interventions vs. trajectories for f_{CP} , f_{Base} , f_{VDN} and ours - $f_{IV(GP+pretrain)}$ (best viewed in color).

We compare f_{VDN} using entropy-based pseudo-labels with $f_{IV(GP)}$ and $f_{IV(IP)}$. The results show that entropy-based labeling doesn’t generalize well across navigators, especially with HAMT, where navigation errors are made with high confidence, causing pseudo-labels to indicate ‘certainty’ even in uncertain cases.

Impact of pre-training MHA in IV (RQ3): It is not feasible to assume that $label_{IP}$ is available for new data used to train f_{IV} . Instead, we leverage instruction-to-path alignment information available from existing data (the FGR2R dataset) to pre-train the Multihead Attention (MHA) network in f_{IV} . Table 2 demonstrates that $f_{IV(GP+pretrain)}$, where f_{IV} is trained with $label_{GP}$ and the MHA was initialized with pre-trained weights, exhibits improvement in SPL, NE and precision-recall balance compared to $f_{IV(GP)}$, which uses an MHA initialized with random weights. These findings indicate that having an MHA network trained on the instruction-to-path alignment task can help enhance its performance in the estimation of instruction vagueness.

Number of oracle interventions: Figure 5 maps the percentage of trajectories to the number of times help was requested within a trajectory when the different models are integrated with DUET. Both f_{Base} and our method reduces the number of questions per trajectory, with our approach requesting more assists than f_{Base} , as expected. Although f_{VDN} has more interventions per trajectory, the lower SPL and NE (see Table 2) achieved despite more number of questions indicate that our approach is more effective in seeking timely assistance.

Qualitative Results (an example with DUET): Figure 4 illustrates an example with the instruction I_{short} : “Go into the room with the French doors”. At time step 4, there is a point of uncertainty because the agent observes two rooms with French doors. At this point, both f_{Base} and f_{VDN} confidently moves to the nearest room with French doors but ends up at the wrong location (red, yellow paths). Our approach (green path) reaches the target after two interventions. In contrast, f_{CP} is overly cautious, seeking assistance at every step (blue path).

5. Conclusion and Future Scope

In this paper, we presented a method to estimate uncertainty from vague instructions in under-specified vision-language navigation tasks. The approach focuses on aligning instructions with the generated path to indicate instruction vagueness. Looking ahead, we aim to further develop this alignment-aware approach to precisely identify “what information is exactly missing”.

6. Acknowledgement

This work was supported by the Centre for Augmented Reasoning, an initiative by the Department of Education, Australian Government.

References

- [1] Peter Anderson, Angel Chang, Devendra Singh Chaplot, Alexey Dosovitskiy, Saurabh Gupta, Vladlen Koltun, Jana Kosecka, Jitendra Malik, Roozbeh Mottaghi, Manolis Savva, et al. On evaluation of embodied navigation agents. *arXiv preprint arXiv:1807.06757*, 2018. 6
- [2] Peter Anderson, Qi Wu, Damien Teney, Jake Bruce, Mark Johnson, Niko Sünderhauf, Ian Reid, Stephen Gould, and Anton Van Den Hengel. Vision-and-language navigation: Interpreting visually-grounded navigation instructions in real environments. In *Proceedings of the IEEE conference on computer vision and pattern recognition*, pages 3674–3683, 2018. 1, 2, 5
- [3] Shizhe Chen, Pierre-Louis Guhur, Cordelia Schmid, and Ivan Laptev. History aware multimodal transformer for vision-and-language navigation. *Advances in neural information processing systems*, 34:5834–5847, 2021. 2, 6
- [4] Shizhe Chen, Pierre-Louis Guhur, Makarand Tapaswi, Cordelia Schmid, and Ivan Laptev. Learning from unlabeled 3d environments for vision-and-language navigation. In *European Conference on Computer Vision*, pages 638–655. Springer, 2022. 2
- [5] Shizhe Chen, Pierre-Louis Guhur, Makarand Tapaswi, Cordelia Schmid, and Ivan Laptev. Think global, act local: Dual-scale graph transformer for vision-and-language navigation. In *Proceedings of the IEEE/CVF Conference on Computer Vision and Pattern Recognition*, pages 16537–16547, 2022. 2, 6
- [6] Hideki Deguchi, Kazuki Shibata, and Shun Taguchi. Language to map: Topological map generation from natural language path instructions. *arXiv preprint arXiv:2403.10008*, 2024. 2
- [7] Mengfei Du, Binhao Wu, Jiwen Zhang, Zhihao Fan, Zejun Li, Ruipu Luo, Xuanjing Huang, and Zhongyu Wei. Delan: Dual-level alignment for vision-and-language navigation by cross-modal contrastive learning. *arXiv preprint arXiv:2404.01994*, 2024. 2
- [8] Weixi Feng, Tsu-Jui Fu, Yujie Lu, and William Yang Wang. Uln: Towards underspecified vision-and-language navigation. *arXiv preprint arXiv:2210.10020*, 2022. 2, 3, 4, 5, 6
- [9] Daniel Fried, Ronghang Hu, Volkan Cirik, Anna Rohrbach, Jacob Andreas, Louis-Philippe Morency, Taylor Berg-Kirkpatrick, Kate Saenko, Dan Klein, and Trevor Darrell. Speaker-follower models for vision-and-language navigation. *Advances in neural information processing systems*, 31, 2018. 2
- [10] Yicong Hong, Cristian Rodriguez-Opazo, Qi Wu, and Stephen Gould. Sub-instruction aware vision-and-language navigation. *arXiv preprint arXiv:2004.02707*, 2020. 5
- [11] Zhiheng Huang, Wei Xu, and Kai Yu. Bidirectional lstm-crf models for sequence tagging. *arXiv preprint arXiv:1508.01991*, 2015. 5
- [12] Balaji Lakshminarayanan, Alexander Pritzel, and Charles Blundell. Simple and scalable predictive uncertainty estimation using deep ensembles. *Advances in neural information processing systems*, 30, 2017. 3
- [13] Ilya Loshchilov and Frank Hutter. Decoupled weight decay regularization. *arXiv preprint arXiv:1711.05101*, 2017. 6
- [14] Fausto Milletari, Nassir Navab, and Seyed-Ahmad Ahmadi. V-net: Fully convolutional neural networks for volumetric medical image segmentation. In *2016 fourth international conference on 3D vision (3DV)*, pages 565–571. Ieee, 2016. 5
- [15] Jeongeun Park, Seungwon Lim, Joonhyung Lee, Sangbeom Park, Minsuk Chang, Youngjae Yu, and Sungjoon Choi. Clara: classifying and disambiguating user commands for reliable interactive robotic agents. *IEEE Robotics and Automation Letters*, 2023. 3
- [16] Yuankai Qi, Qi Wu, Peter Anderson, Xin Wang, William Yang Wang, Chunhua Shen, and Anton van den Hengel. Reverie: Remote embodied visual referring expression in real indoor environments. In *Proceedings of the IEEE/CVF Conference on Computer Vision and Pattern Recognition*, pages 9982–9991, 2020. 1
- [17] Yanyuan Qiao, Yuankai Qi, Zheng Yu, Jing Liu, and Qi Wu. March in chat: Interactive prompting for remote embodied referring expression. In *Proceedings of the IEEE/CVF International Conference on Computer Vision*, pages 15758–15767, 2023. 2
- [18] Niyati Rawal, Roberto Bigazzi, Lorenzo Baraldi, and Rita Cucchiara. Aigen: An adversarial approach for instruction generation in vln. In *Proceedings of the IEEE/CVF Conference on Computer Vision and Pattern Recognition*, pages 2070–2080, 2024. 2
- [19] Allen Z Ren, Anushri Dixit, Alexandra Bodrova, Sumeet Singh, Stephen Tu, Noah Brown, Peng Xu, Leila Takayama, Fei Xia, Jake Varley, et al. Robots that ask for help: Uncertainty alignment for large language model planners. *arXiv preprint arXiv:2307.01928*, 2023. 3, 6
- [20] David E Rumelhart, Geoffrey E Hinton, and Ronald J Williams. Learning representations by back-propagating errors. *nature*, 323(6088):533–536, 1986. 4
- [21] Ilya Sutskever, Oriol Vinyals, and Quoc V Le. Sequence to sequence learning with neural networks. *Advances in neural information processing systems*, 27, 2014. 5
- [22] Jesse Thomason, Michael Murray, Maya Cakmak, and Luke Zettlemoyer. Vision-and-dialog navigation. In *Conference on Robot Learning*, pages 394–406. PMLR, 2020. 3
- [23] Ashish Vaswani, Noam Shazeer, Niki Parmar, Jakob Uszkoreit, Llion Jones, Aidan N Gomez, Łukasz Kaiser, and Illia Polosukhin. Attention is all you need. *Advances in neural information processing systems*, 30, 2017. 3
- [24] Xiaohan Wang, Wenguan Wang, Jiayi Shao, and Yi Yang. Lana: A language-capable navigator for instruction following and generation. In *Proceedings of the IEEE/CVF Conference on Computer Vision and Pattern Recognition*, pages 19048–19058, 2023. 2
- [25] Wansen Wu, Tao Chang, Xinmeng Li, Quanjun Yin, and Yue Hu. Vision-language navigation: a survey and taxonomy. *Neural Computing and Applications*, 36(7):3291–3316, 2024. 1
- [26] Yue Zhang, Quan Guo, and Parisa Kordjamshidi. Navhint: Vision and language navigation agent with a hint generator. *arXiv preprint arXiv:2402.02559*, 2024. 2

- [27] Gengze Zhou, Yicong Hong, and Qi Wu. Navgpt: Explicit reasoning in vision-and-language navigation with large language models. In *Proceedings of the AAAI Conference on Artificial Intelligence*, volume 38, pages 7641–7649, 2024. [2](#)
- [28] Yi Zhu, Yue Weng, Fengda Zhu, Xiaodan Liang, Qixiang Ye, Yutong Lu, and Jianbin Jiao. Self-motivated communication agent for real-world vision-dialog navigation. In *Proceedings of the IEEE/CVF International Conference on Computer Vision*, pages 1594–1603, 2021. [3](#), [6](#)